Electronic Supplementary Material (ESI) for Environmental Science: Nano.

Supplementary Materials

Recovery and separation of uranium in a microbial fuel cell using a titanium dioxide nanotube array cathode

Wenbin Liu[a,b], Leiming Lin[a,b], Ying Meng[a], Ziwang Zhao[a,b], Yahua Wang[a,b], and Fubo Luan[a,b]*

[a] Key Laboratory of Drinking Water Science and Technology, Research Center for Eco-Environmental Sciences, Chinese Academy of Sciences, Beijing 100085, PR China

[b] University of Chinese Academy of Sciences, Beijing 100049, PR China

*Corresponding author:

E-mail: fbluan@rcees.ac.cn

Number of Pages: 15

Number of Texts: 1

Number of Figures: 13

Number of Tables: 7

Text S1

The two-chamber MFC used in this study was separated by a piece of proton exchange membrane (PEM, NafionTM 117, Dupont Co, USA) that had a surface area of 7 cm^2 (diameter=3 cm). The PEM was pretreated as described by Liu and Logan.[1] Carbon fiber brush electrode (length=3.0 cm, diameter=2.5 cm) was used as anode and cathode during the startup period.

The anode chamber was inoculated with 30 mL effluent (containing adapted microbial consortium) from other well established MFCs operated for about one year in our lab and 120 ml anolyte medium. The anolyte medium contained the following components chemicals (per liter): sodium acetate, 1.0 g; NH_4Cl, 0.2 g; $CaCl_2$, 0.12g; KCl, 0.33 g; NaCl, 0.30 g; $MgCl_2 \cdot 6H_2O$, 6.73 g; K_2HPO_4, 1.26 g; KH_2PO_4, 0.42g; trace metals (1 ml) and vitamin (1 ml). The initial pH of the anolyte was adjusted to 7.0 using 10% (wt%) HCl and 10 M NaOH. During the startup period, potassium ferricyanide (20 mM) was used as the terminal electron acceptor.

The MFC was started up when the voltage across the resistor (1000 Ω) can repeatedly increase to a level of 500 mV after change electrolytes, and the anode potential was lower than –0.300 V (vs NHE).

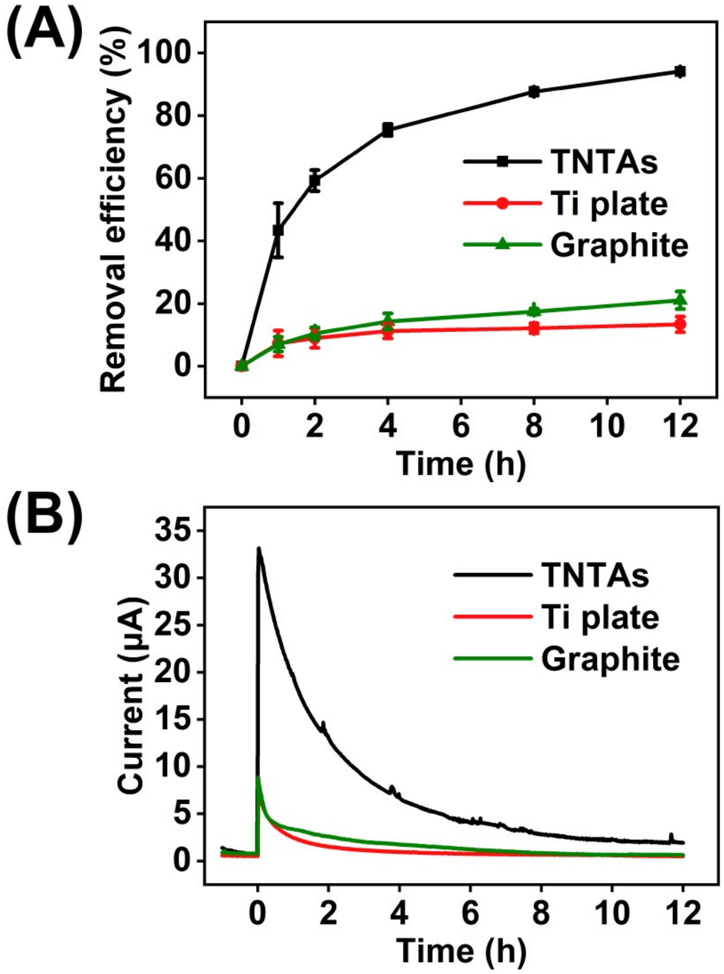

Fig. S1 Bioelectro-removal of U(VI) in MFC using TNTAs, Ti plate, and graphite as cathode. Experiments were conducted with 10 μM U(VI), 1 mM Ca^{2+}, 2 mM HCO_3^- at pH 7.0. (A) The removal efficiency of U(VI) versus time. (B) The bioelectro-reduction current versus time.

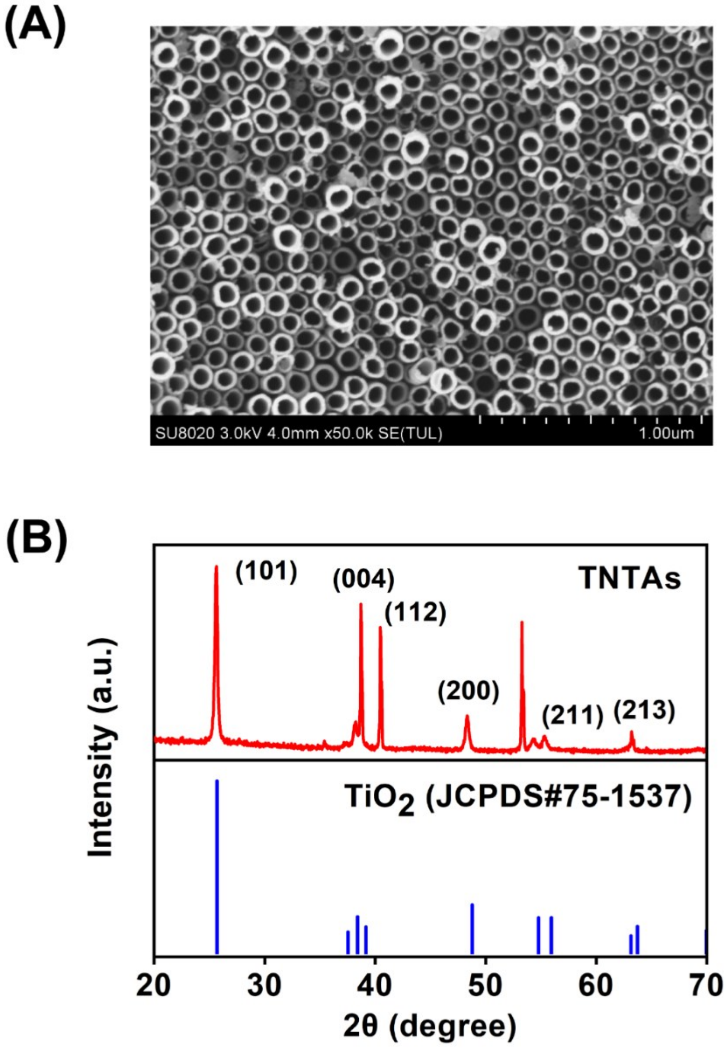

Fig. S2 The SEM image (A) and XRD pattern (B) of the TNTAs cathode prepared by the electrochemical anodic oxidation method.

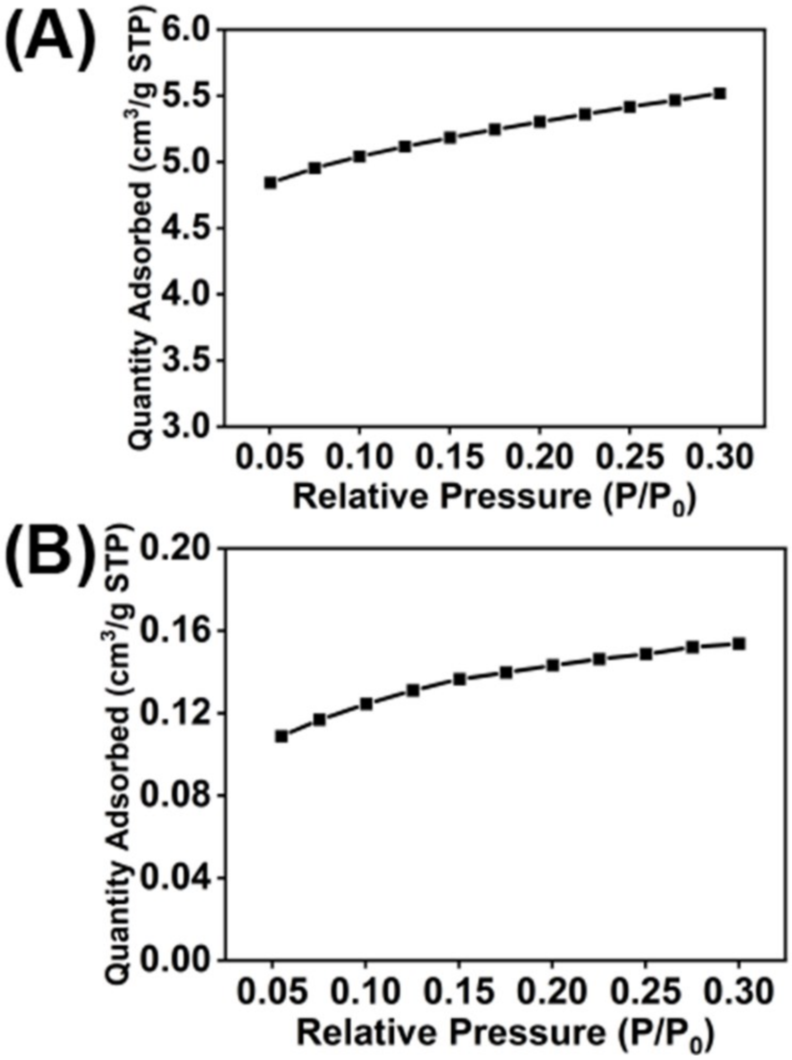

Fig. S3 The N_2 adsorption isotherm recorded as volume of gas adsorbed (cm^3/g STP) versus relative pressure (P/P_0). (A) TNTAs electrode. (B) Ti plate electrode.

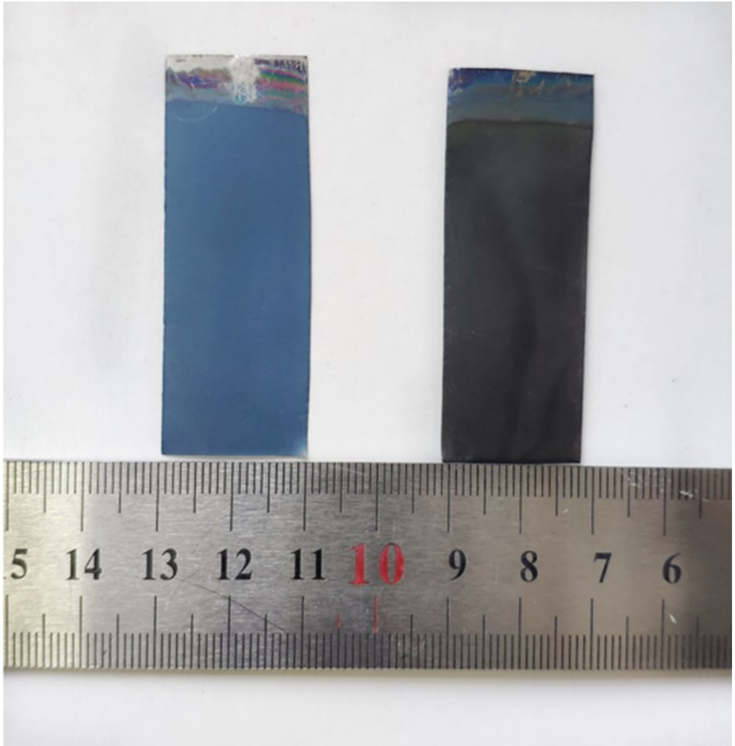

Fig. S4 The TNTAs cathode before (left) and after (right) bioelectro-reduction of U(VI) in MFC.

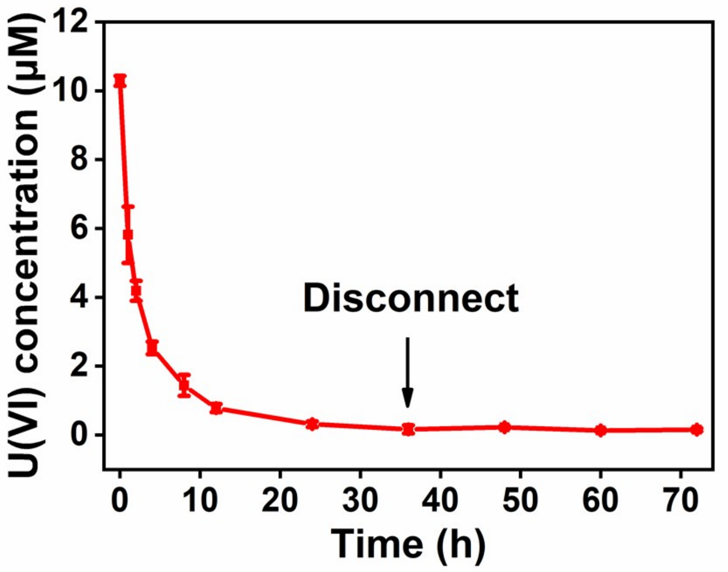

Fig. S5 Removal of U(VI) (10 μM) in MFC and no release of U(VI) was observed when the external circuit was disconnected after 36 hours.

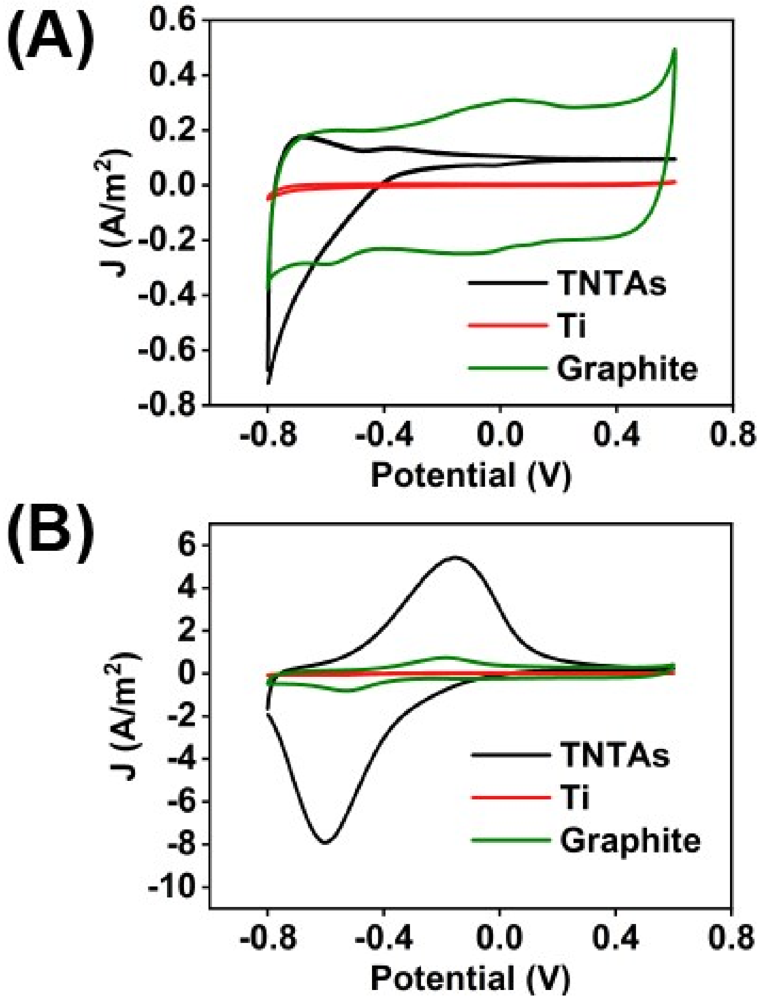

Fig. S6 Cyclic voltammetry of different cathode material (TNTAs, Ti plate, and Graphite). (A) In the absence U(VI) and (B) In the presence of 10 µM U(VI).

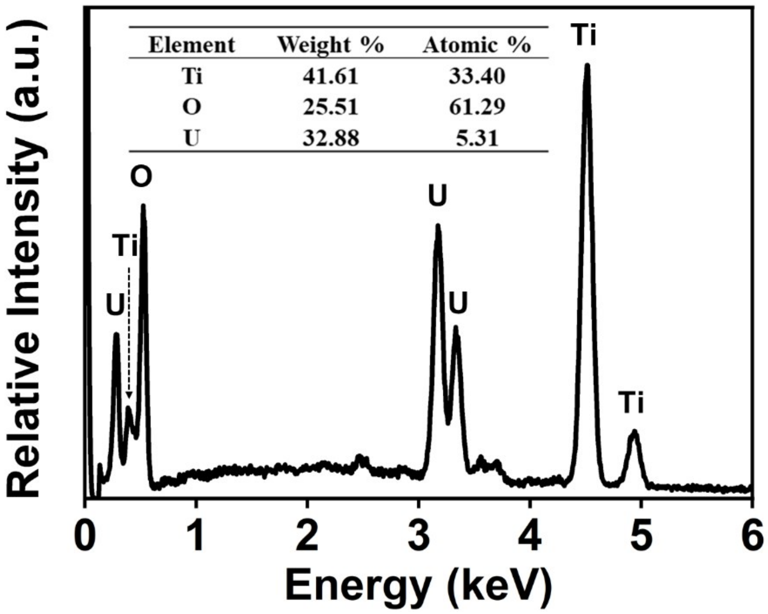

Element	Weight %	Atomic %
Ti	41.61	33.40
O	25.51	61.29
U	32.88	5.31

Fig. S7 The EDS spectra for the deposits.

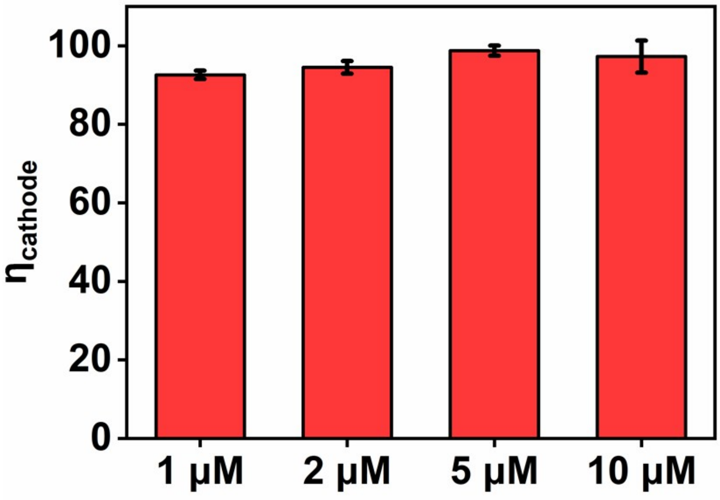

Fig. S8 The $\eta_{cathode}$ of MFC at different initial U(VI) concentrations (1 − 10 μM).

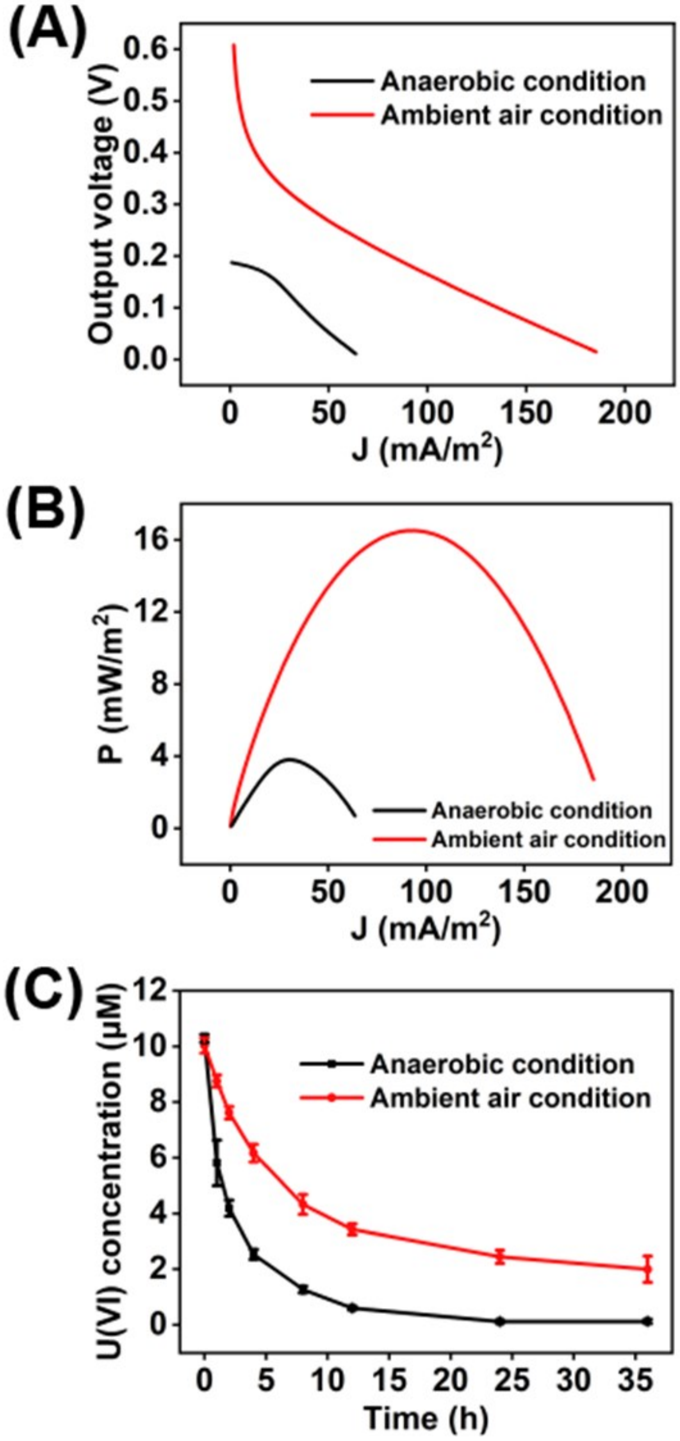

Fig. S9 Bioelectro-removal of 10 μM U(VI) using TNTAs under anaerobic and ambient air conditions ($[Ca^{2+}]$=1 mM, $[HCO_3^-]$=2 mM and pH=7.0). (A) Output voltage as a function of current density (J). (B) Power density (P) as a function of current density (J). (C) U(VI) concentration versus time.

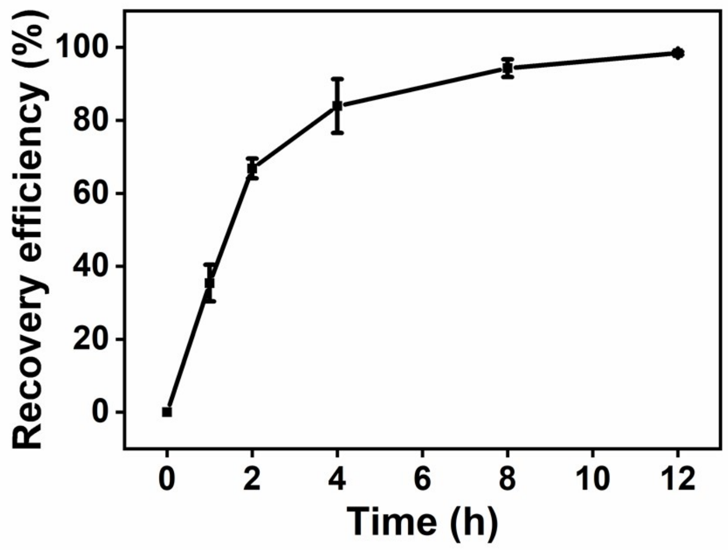

Fig. S10 Uranium separation from the TNTAs cathode in 2% HNO_3 solution.

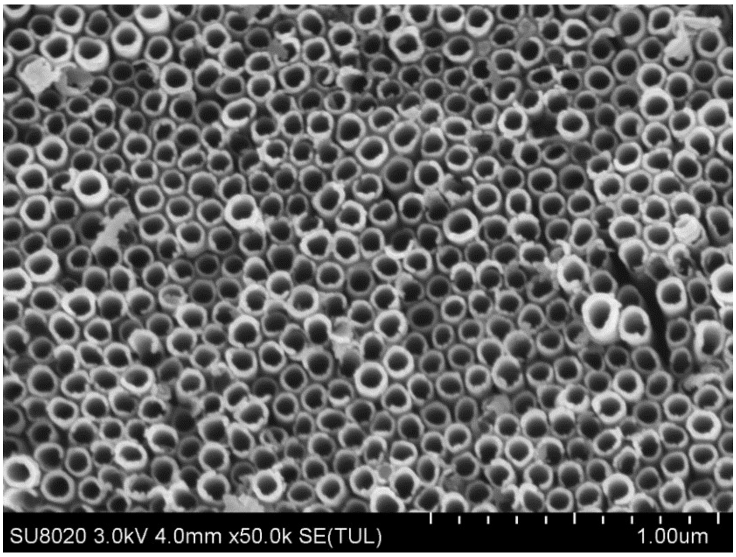

Fig. S11 The SEM image of used TNTAs cathode after five cycles of removal and separation of uranium.

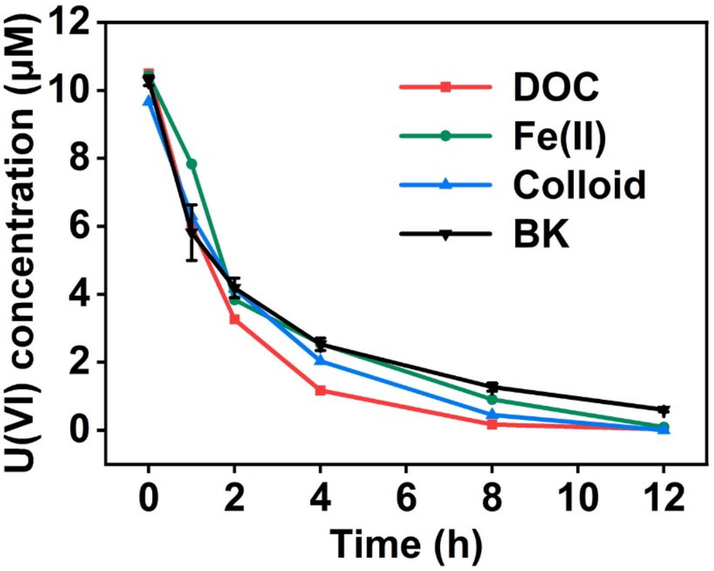

Fig. S12 Effect of dissolved organic carbon (DOC), dissolved Fe(II) and colloid on the bioelectro-removal of U(VI). Experiments were conducted with 10 μM U(VI).

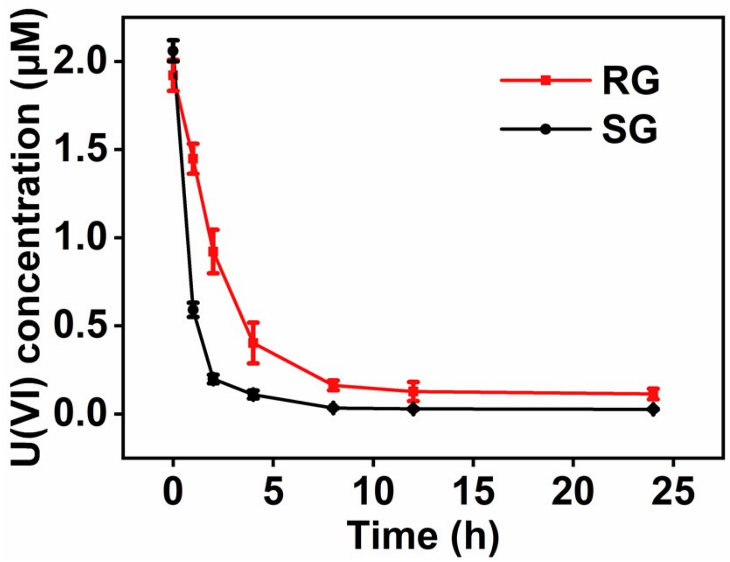

Fig. S13 Bioelectro-removal of U(VI) from real uranium-containing groundwater and simulated uranium-containing groundwater.

Table S1. The constituents of simulated uranium-containing groundwater (SG).

Constituents	Concentration (mM)
U(VI)	0.001 – 0.01
$NaHCO_3$	2 – 40
$CaCl_2$	0 – 3
PIPES/HEPES buffer	30

Table S2. The constituents of real uranium-containing groundwater (RG) from Shandong province of China.

Constituents	Concentration (mM)
U(VI)	0.00192 ± 0.00009
NO_3^-	0.81 ± 0.001
SO_4^{2-}	1.94 ± 0.25
CO_3^{2-}	1.00 ± 0.01
Na^+	1.06 ± 0.03
Mg^{2+}	1.13 ± 0.04
K^+	0.10 ± 0.005
Ca^{2+}	1.07 ± 0.06

Table S3. The mixture ratio of N_2 and CO_2 under different experiment conditions.

pH	Bicarbonate (mM)	Mixture ratio (N_2:CO_2)
7.0	2.0	1:99
7.0	10.0	5:99
7.0	40.0	20:80
6.0	2.0	10:90
7.5	2.0	0.3:99.7
8.0	2.0	0.1:99.9

Table S4. The dominant U(VI) species at different initial U(VI) concentrations.

Uranium (μM)	Dominant U(VI) species	The proportion of U(VI) species (%)
1	$Ca_2UO_2(CO_3)_3$	65.59
	$CaUO_2(CO_3)_3^{2-}$	32.08
2	$Ca_2UO_2(CO_3)_3$	65.55
	$CaUO_2(CO_3)_3^{2-}$	32.11
5	$Ca_2UO_2(CO_3)_3$	64.43
	$CaUO_2(CO_3)_3^{2-}$	32.19
10	$Ca_2UO_2(CO_3)_3$	65.22
	$CaUO_2(CO_3)_3^{2-}$	32.32

Table S5. The proportion of dominant U(VI) species and their electrode potential (vs NHE) under different conditions. The Gibbs Free Energy of formation for species used in the thermodynamic calculations were collected from previous studies.[2, 3]

HCO_3^- (mM)	Ca^{2+} (mM)	pH	Proportion of dominate U(VI) species	Electrode potential (V vs NHE)
2	0	7.0	$(UO_2)_2CO_3(OH)_3^-$ (48.00%)	0.123
10	0	7.0	$UO_2(CO_3)_3^{4-}$ (56.79%)	0.089
40	0	7.0	$UO_2(CO_3)_3^{4-}$ (91.98%)	0.035
2	0.5	7.0	$Ca_2UO_2(CO_3)_3$ (48.49%)	0.092
2	1	7.0	$Ca_2UO_2(CO_3)_3$ (65.22%)	0.075
2	3	7.0	$Ca_2UO_2(CO_3)_3$ (82.50%)	0.046
2	1	6.0	$Ca_2UO_2(CO_3)_3$ (41.64%)	0.163
2	1	7.5	$Ca_2UO_2(CO_3)_3$ (66.25%)	0.030
2	1	8.0	$Ca_2UO_2(CO_3)_3$ (66.30%)	–0.014

Table S6. The U(VI) species and their proportions of real uranium-containing groundwater.

U(VI) species	Proportions (%)
$Ca_2UO_2(CO_3)_3$	66.94
$CaUO_2(CO_3)_3^{2-}$	31.70
$UO_2(CO_3)_2^{2-}$	0.86
$UO_2(CO_3)_3^{4-}$	0.37
UO_2CO_3 (aq)	0.119

Table S7. The U(VI) complexation constants used in the speciation simulations.

Reaction	log *K*
$2UO_2^{2+} + CO_3^{2-} + 3H_2O \leftrightarrow (UO_2)_2CO_3(OH)_3^{-} + 3H^{+}$	–0.86
$UO_2^{2+} + CO_3^{2-} \leftrightarrow UO_2CO_3(aq)$	9.94
$UO_2^{2+} + 2CO_3^{2-} \leftrightarrow UO_2(CO_3)_2^{2-}$	16.61
$UO_2^{2+} + 3CO_3^{2-} \leftrightarrow UO_2(CO_3)_3^{4-}$	21.84
$UO_2^{2+} + Ca^{2+} + 3CO_3^{2-} \leftrightarrow CaUO_2(CO_3)_3^{2-}$	27.18
$UO_2^{2+} + 2Ca^{2+} + 3CO_3^{2-} \leftrightarrow Ca_2UO_2(CO_3)_3$	30.7

References

1. H. Liu and B. E. Logan, Electricity generation using an air-cathode single chamber microbial fuel cell in the presence and absence of a proton exchange membrane, *Environ. Sci. Technol.*, 2004, **38**, 4040-4046.
2. M. Ginder-Vogel, C. S. Criddle and S. Fendorf, Thermodynamic constraints on the oxidation of biogenic UO_2 by Fe(III)(hydr) oxides, *Environ. Sci. Technol.*, 2006, **40**, 3544-3550.
3. R. Guillaumont and F. J. Mompean, *Update on the chemical thermodynamics of uranium, neptunium, plutonium, americium and technetium*, Elsevier Amsterdam, 2003.